HHS Public Access

Author manuscript

Mol Imaging Biol. Author manuscript; available in PMC 2021 March 13.

Published in final edited form as:

Mol Imaging Biol. 2020 February ; 22(1): 181–189. doi:10.1007/s11307-019-01376-9.

Semiquantitative Parameters in PSMA-Targeted PET Imaging with [^{18}F]DCFPyL: Intrapatient and Interpatient Variability of Normal Organ Uptake

Karine Sahakyan[#1], **Xin Li**[#2], **Martin A. Lodge**[1], **Rudolf A. Werner**[1,3,4], **Ralph A. Bundschuh**[5], **Lena Bundschuh**[5], **Harshad R. Kulkarni**[6], **Christiane Schuchardt**[6], **Richard P. Baum**[6], **Kenneth J. Pienta**[7], **Martin G. Pomper**[1,7], **Ashley E. Ross**[8], **Michael A. Gorin**[1,7], **Steven P. Rowe**[1,7,9]

[1]The Russell H. Morgan Department of Radiology and Radiological Science, Johns Hopkins University School of Medicine, Baltimore, MD, USA

[2]Department of Nuclear Medicine, Qilu Hospital, Shandong University, Jinan City, Shandong Province, China

[3]Department of Nuclear Medicine and Comprehensive Heart Failure Center, University Hospital Wuerzburg, Wuerzburg, Germany

[4]Department of Nuclear Medicine, Hannover Medical School, Hannover, Germany

[5]Department of Nuclear Medicine, University Medical Center Bonn, Bonn, Germany

[6]Theranostics Center for Molecular Radiotherapy and Molecular Imaging, Zentralklinik Bad Berka, Bad Berka, Germany

[7]The James Buchanan Brady Urological Institute and Department of Urology, Johns Hopkins University School of Medicine, Baltimore, MD, USA

[8]Texas Urology Specialists, Dallas, TX, USA

[9]Division of Nuclear Medicine and Molecular Imaging, The Russell H. Morgan Department of Radiology and Radiological Science, Johns Hopkins University School of Medicine, 600 N. Wolfe St., Baltimore, MD, 21287, USA

[#] These authors contributed equally to this work.

Abstract

Correspondence to: Steven Rowe; srowe8@jhmi.edu.

Electronic supplementary material The online version of this article (https://doi.org/10.1007/s11307-019-01376-9) contains supplementary material, which is available to authorized users.

Conflict of interest

Martin G. Pomper is a co-inventor on a patent covering [^{18}F]DCFPyL and is entitled to a portion of any licensing fees and royalties generated by this technology. This arrangement has been reviewed and approved by the Johns Hopkins University in accordance with its conflict-of-interest policies. He has also received research funding from Progenics Pharmaceuticals, the licensee of ^{18}F-DCFPyL. Michael A. Gorin has served as a consultant to, and has received research funding from, Progenics Pharmaceuticals. Kenneth J. Pienta has received research funding from Progenics Pharmaceuticals. Steven P. Rowe has received research funding from Progenics Pharmaceuticals.

Purpose: Prostate-specific membrane antigen (PSMA)-targeted positron emission tomography (PET) imaging has impacted the management of patients with prostate cancer (PCa) in many parts of the world. PSMA-targeted endoradiotherapies are also being increasingly utilized and for these applications, the radiopharmaceutical distribution in normal organs is particularly important because it may limit the dose that can be delivered to tumors. In this study, we measured both interpatient and intrapatient variability of [^{18}F]DCFPyL uptake in the most relevant normal organs.

Procedures: Baseline and 6-month follow-up PSMA-targeted [^{18}F]DCFPyL PET/computed tomography (CT) scans from 39 patients with PCa were reviewed. Volumes of interest were manually drawn using the best visual approximation of the organ edge for both lacrimal glands, all four major salivary glands, the liver, the spleen, and both kidneys for all patients. The average SUV_{mean}, the COVs, and intraclass correlation coefficients (ICCs) across scans were calculated. Bland-Altman analyses were performed for all organs to derive repeatability coefficients (RCs).

Results: The liver demonstrated the lowest interpatient variability (13.0 and 16.6 % at baseline and follow-up, respectively), while the spleen demonstrated the largest interpatient variability (44.6 and 51.0 % at baseline and follow-up, respectively). The lowest intrapatient variability was found in the spleen (ICC 0.86) while the highest intrapatient variability was in the kidneys (ICCs 0.40–0.50). Bland-Altman analyses showed 95 % repeatability coefficients for mean uptake >40 % for multiple organs and were highest for the lacrimal glands, kidneys, and spleen.

Conclusions: Normal organs demonstrate significant variability in uptake of the PSMA-targeted radiotracer [^{18}F]DCFPyL. Depending on the organ, different contributions of interpatient and intrapatient factors affect the intrinsic variability. The RCs also vary significantly among the different organs were highest for the lacrimal glands, kidneys, and spleen. These findings may have important implications for the design of clinical protocols and personalized dosimetry for PSMA-targeted endoradiotherapies.

Keywords

Prostate-specific membrane antigen; Prostate cancer; Endoradiotherapy; Radioligand therapy

Introduction

In recent years, positron emission tomography (PET) imaging of prostate cancer (PCa) with small-molecule ligands that target prostate-specific membrane antigen (PSMA) have come into common use throughout much of the world and these agents have found applications across a range of clinical contexts [1–3]. Clinical decision-making is often impacted by findings on PSMA-targeted PET scans [4–6], and PSMA-targeted endoradiotherapeutics are being increasingly utilized in the treatment of advanced disease [7–9]. For both diagnostic and therapeutic applications, a clear understanding of the normal biodistributions of radiotracers and their expected variations are important [10].

We have previously reported on normal organ uptake variability in 65 consecutive PET scans obtained with the PSMA-targeted small-molecule radiotracer [^{18}F]DCFPyL [11]. Of note, the interpatient variability of liver uptake in that patient cohort was the lowest of any of the investigated normal organs, and was less than the degree of variability seen with the more

commonly used oncology radiotracer 2-deoxy-2-[^{18}F]fluoro-D-glucose ([^{18}F]FDG) [11]. However, a number of questions remained unanswered after that study. First, this study involved imaging on only one occasion (only one patient was imaged twice), and therefore the stability of uptake in normal organs in individual patients at different time points was not investigated. Second, both interpatient (*e.g.*, differences in weight, height, body composition, medical comorbidities, differences in prior therapies for PCa, *etc.*) and intrapatient (*e.g.*, time of day, recent meals, intercurrent therapies, *etc.*) sources of variability exist, and the contributions of these two groups of disparate factors to the overall variability was unknown. Indeed, since the time of our initial study, Wondergem et al. have described significantly higher uptake of [^{18}F]DCFPyL in normal organs in patients who are non-fasting *versus* those who are fasting [12], confirming that perturbations in intrapatient sources of variability can alter the quantitative biodistribution of PSMA-targeted radiotracers. As new PSMA-targeted endoradiotherapeutics are used more commonly in clinical practice, particularly α-particle emitting agents [9], it will be necessary to understand the variability in uptake that occurs in normal organs to predict and decrease off-target radioactive dose and potential associated toxicities.

We have therefore sought to further investigate the stability of normal organ radiotracer uptake in a series of PCa patients who had two [^{18}F]DCFPyL PET/computed tomography (CT) scans, separated in time by approximately 6 months, so as to assess the intrinsic stability of PSMA-targeted radiotracer uptake in normal organs and to differentiate the relative aggregate contributions of interpatient and intrapatient sources of variability. An understanding of these factors may serve as a hypothesis-generating mechanism for further study into more specific aspects of normal organ variability with PSMA-targeted radiotracers.

Materials and Methods

Patient Population

We retrospectively reviewed consecutive baseline [^{18}F]DCFPyL PET/CT scans acquired between June 2015 and November 2015 of 39 patients with history of PCa who had all undergone radical prostatectomy and were then subsequently found to have an elevated prostate-specific antigen (PSA) level (≥ 0.2 ng/ml). All 39 patients also had follow-up [^{18}F]DCFPyL PET/CT scans performed between October 2015 and July 2016. All patients were imaged on a prospective, institutional review board-approved protocol investigating [^{18}F]DCFPyL (ClinicalTrials.gov identifier NCT02523924), and all gave written informed consent before undergoing imaging. This study was conducted under the auspices of a United States Food and Drug Administration Investigational New Drug Application (IND 121064).

Image Acquisition and Analysis

[^{18}F]DCFPyL was produced according to current good manufacturing practices using previously described radiosynthetic methodologies [13, 14]. The patients fasted, except for medication and water, for 4–6 h before injection of radiotracer, as per our usual clinical protocol. Approximately 1 h after the intravenous injection of ≤ 333 MBq (≤9 mCi)

[^{18}F]DCFPyL, PET images were acquired over 6–8 bed positions from the mid-thighs to the skull vertex (depending on patient height) with the patients in the supine position. The acquisitions were performed on either a Discovery RX 64-slice PET/CT scanner (General Electric, Waukesha, WI, USA) or a Biograph mCT 128-slice PET/CT scanner (Siemens, Erlangen, Germany) as part of standard work-flow in our PET center. Both scanners were operated in 3D emission mode with CT attenuation correction. Image reconstruction was performed with the standard clinical ordered subset expectation maximization algorithms available on the scanners.

PET images were analyzed using the XD3 Software (Mirada Medical, Oxford, UK), which allowed simultaneous review of PET, CT, and fused PET/CT image data. Volumes of interest (VOIs) were manually drawn over entire normal organ volumes using the best visual approximation of the organ edge as has previously been described [11, 15]. Given the biodistribution of the radiotracer (Fig. 1), these VOIs included both lacrimal glands, all four major salivary glands (two parotid glands and two submandibular glands), the liver, the spleen, and both kidneys for all patients. The same parameters were also derived for a 3-cm sphere drawn in the center of the right hepatic lobe. Mean standardized uptake values (SUV_{mean}) were recorded for all organs, corrected for body weight. Body weight correction was chosen due to simplicity of calculation relative to lean body mass correction and the results of our prior work that demonstrated no correlation between calculated uptake values and either body weight or lean body mass [11].

Statistical Analysis

Descriptive statistics were calculated mean values with standard deviations. From repeated measures over time, coefficients of variation (COVs) and intraclass correlation coefficients (ICCs) across scans for the same patient and across all scans from all patients were calculated using variance estimates obtained through analysis of variance (ANOVA). Additionally, ICCs were calculated using the method described by Shrout and Fleiss [16]. For reference, interpretation of ICCs is commonly categorized as 0.41–0.60 = moderate reproducibility, 0.61–0.80 = substantial reproducibility, and 0.81–1.00 = almost-perfect reproducibility [17]. Percentage change in SUV mean for each normal organ uptake between baseline and follow-up scan was calculated. Bland-Altman plots were constructed to display percentage difference between two measurements *versus* their average. Relative units (*i.e.*, percentages as opposed to absolute units) were utilized for the Bland-Altman analysis because the normal organ uptake differences between the two scans were proportional to the absolute uptake [18, 19]. Data were analyzed using the SAS 9.3 software (SAS Institute, Inc., Cary, NC, USA).

Results

Patient Population

Selected demographic and clinical information from the patient cohort in this study is presented in Supplementary Table 1. Mean time between scans was 211 days (standard deviation 33 days). Mean age of patients was 62.9 years (standard deviation 6.8 years). Thirty-five patients were Caucasian (89.7 %), two were African-American (5.1 %), and two

(5.1 %) did not disclose their race. Most patients were found to have an elevated PSA level in a relatively short timeframe following prostatectomy, with 21 of 39 patients (53.9 %) being imaged at 3 to 16 months postoperatively. The mean serum PSA levels at the time of first imaging was 2.7 ± 5.3 ng/ml. A number of therapies were utilized between the baseline and follow-up imaging, with only 3/39 (7.7 %) patients being observed without any additional therapy (see Suppl. Table 1, see Electronic Supplementary Material). As noted above, patients were scanned on one of two calibrated clinical scanners; no significant difference was found between the liver SUV_{mean} generated by each scanner, as discussed in detail in the Electronic Supplementary Material.

Image and Statistical Analyses

Table 1 demonstrates mean SUV_{mean} with standard deviations for each organ at baseline and follow-up. The highest recorded SUV_{mean} were in the kidneys (left kidney 19.6 ± 4.5 at baseline and 17.4 ± 4.9 at follow-up and right kidney baseline 20.4 ± 4.7 and 17.9 ± 5.4 at follow-up) followed by the submandibular glands (left submandibular gland 9.4 ± 2.0 at baseline and 8.9 ± 2.1 at follow-up and right submandibular gland 9.6 ± 2.1 at baseline and 8.9 ± 2.1 at follow-up) and the parotid glands (left parotid gland 8.8 ± 1.9 at baseline and 8.4 ± 1.6 at follow-up and right parotid gland 8.8 ± 1.8 at baseline and 8.2 ± 1.6 at follow-up). Taken together with the lacrimal glands (left lacrimal gland 6.2 ± 1.9 at baseline and 6.2 ± 1.5 at follow-up and right lacrimal gland 6.5 ± 2.0 at baseline and 6.2 ± 1.8 at follow-up), all of the paired organs demonstrated very similar overall uptake, suggesting that the VOIs were reliably drawn. The lowest mean SUV_{mean} were detected in the spleen (4.1 ± 1.8 at baseline and 4.3 ± 2.2 at follow-up) followed by the liver (5.0 ± 0.7 at baseline and 5.2 ± 0.9 at follow-up). In 7/10 (70.0 %) organs included in the analysis, the mean SUV_{mean} decreased from the baseline to the follow-up scan, although in all cases the ranges of the SUV_{mean} at each time point considerably overlapped for each. Nonetheless, both kidneys and the right submandibular gland demonstrated significantly lower uptake at the second time point (Table 1, p values < 0.05).

The calculated COVs and ICCs are shown in Table 2. Consistent with our prior results [11], the liver was the organ demonstrating the lowest variability across all patients (*i.e.*, the lowest COV) at either time point (COVs of 13.0 and 16.6 % at baseline and on follow-up, respectively). The spleen demonstrated the highest variability across all scans at either time point (COVs of 44.6 and 51.0 % at baseline and on follow-up, respectively). The kidneys, lacrimal glands, parotid glands, and submandibular glands all demonstrated intermediate levels of variability across scans, with COVs ranging between 19.4 and 31.3 % (Table 2).

Figures 2, 3, 4 show the Bland-Altman plots described in the “Materials and Methods” section of the manuscript. Table 3 summarizes the mean percentage differences in uptake and 95 % confidence limits (repeatability coefficients (RCs)) for maximal percentage differences in uptake of the various organs. The kidneys demonstrated the highest percentage mean differences in uptake (left kidney mean percentage difference +10.1 % and right kidney mean percentage difference +9.9 % (Table 3)). The lacrimal glands, kidneys, and spleen demonstrated the widest RCs (left lacrimal gland 95 % confidence upper limit +41.9 % and 95 % lower confidence limit −40.5 %; right lacrimal gland 95 % confidence upper

limit +47.8 % and 95 % lower confidence limit −38.3 %; left kidney 95 % confidence upper limit +41.3 % and 95 % confidence lower limit −21.1 %; right kidney 95 % confidence upper limit +45.0 % and 95 % confidence lower limit −25.2 %; spleen 95 % confidence upper limit +41.3 % and 95 % confidence lower limit −46.5 % (Table 3)). Although the mean percentage differences of other organs are in the range of −2.7 to +8.1 %, all have RCs > 20 % (Table 3).

In regard to whether the sources of variability were related to intrapatient or interpatient factors, the liver and right parotid gland demonstrated moderate intrapatient variability (ICCs 0.40–0.57), whereas all other organs had lower levels of intrapatient variability (Table 2). Indeed, relatively low intrapatient variability was demonstrated in the lacrimal glands (ICCs 0.72 each, respectively) and submandibular glands (ICCs 0.73–0.74), although the lowest intrapatient variability was calculated for the normal spleen (ICC 0.86) (Table 3).

Discussion

In this patient cohort, significant variability was found in normal organ uptake between [^{18}F]DCFPyL PET scans that were performed approximately 6 months apart and with many patients receiving therapy in between the scans. While our study was conducted with [^{18}F]DCFPyL, the generally similar biodistribution of many urea-based small-molecule inhibitors of PSMA suggest that the conclusions discussed herein may be applicable to other PSMA-based PET radiotracers.

Overall, the results of this study are consistent with, and expand upon, our prior work on semiquantitative parameters in PSMA-targeted PET [11]. In particular, the COVs calculated for the baseline and follow-up scans for all organs were similar to the previously reported values across 65 consecutive scans as reported by Li et al. [11]. However, with the second time point available in this study, the relative contributions of interpatient and intrapatient factors to the variability in normal organs were calculated. Based on the obtained results, the liver and kidneys (ICCs 0.40–0.57) demonstrate the greatest degree of variability on the basis of intrapatient factors such as time of day, recent meals, hydration status, and therapies occurring during the time interval between scans. In contradistinction, the variability in normal lacrimal glands, salivary glands, and spleen (ICCs 0.58–0.86) are most dependent upon interpatient differences including weight, height, body composition, medical comorbidities, and differences in prior therapies. Of note, on the second time point scan, both kidneys and the right submandibular gland had significantly lower uptake than was measured on the first scan; we speculate that this could be related to the interval therapies that the patients received, although it will require more study to validate whether that is true. It is important to note that the data contained in this manuscript does not address the relative contributions of specific intrapatient and interpatient factors and instead focuses on variability and how it is impacted by intrapatient and interpatient differences in aggregate.

In addition to the interpatient sources of variability, the second time point scans in this study allowed for a Bland-Altman analysis. Although this study is not a true test-retest protocol due to the extended interval between imaging, the findings are nonetheless instructive as to the degree of variability that can occur in normal organs with PSMA-targeted radiotracers.

The RCs for multiple organs were above 40 %, indicating that the amount of uptake in normal organs on a single scan does not always accurately predict the uptake on a subsequent scan in the same patient. This degree of normal organ variability is likely in line with [^{18}F]FDG, as test-retest studies with tumor uptake of that radiotracer have demonstrated RCs as high as 49% [20] and that the limits of repeatability can be asymmetric [21]. The RCs for [^{18}F]DCFPyL in this study may have important implications for PSMA-targeted radiotracers in general. First, for diagnostic PET radiotracers, the dosimetry calculated at a single time point cannot be multiplied to arrive at the dosimetry for multiple scans. Second, the dose to individual organs from PSMA-targeted endoradiotherapeutics may vary substantially across multiple administered doses, suggesting that administered activities may need to be adjusted based on the RCs of the dose-limiting, normal organ for any given endoradiotherapy. Third, further research is necessary to elucidate what interpatient and intrapatient factors contribute to the variability/RCs so that those factors may be manipulated to decrease normal organ uptake in patients undergoing PSMA-targeted endoradiotherapy. Thus, the data presented here may serve as a hypothesis-generating study for investigations into individual factors that significantly impact normal organ uptake and might be leveraged to improve the off-target dosimetry of PSMA-targeted therapeutic agents.

Several important limitations of this study should be noted. Perhaps most noteworthy is the fact that patients in this analysis underwent a wide variety of different therapies between their first and second [^{18}F]DCFPyL PET/CT scans, including four patients who received PSMA-targeted endoradiotherapy. The potential effects of those different therapies on uptake of PSMA-targeted radiotracers in normal organs are unknown. Further, although the patients in this study were participating in a prospective trial, the data in this manuscript are from a retrospective, *post hoc* analysis that was not related to the original reason the patients had been imaged. Although all patients in this study were asked to be *nil per os* (except for medication and water) for 4–6 h prior to imaging at both time points, it is unknown if patients followed those instructions and what affect non-compliance may have had on intrapatient variability. Further, while we have speculated that the findings we have derived with [^{18}F]DCFPyL may be applicable to other, structurally similar radiotracers targeting PSMA, such extrapolation must be made with abundant caution. The development of the compound [^{18}F]PSMA-1007, for example, has highlighted the potential for different biodistributions for otherwise-similar PSMA-targeted agents [22]; this highlights the need for similar studies with other compounds to deepen the understanding of normal organ variability in the context of this important new class of radiotracers. Also, due to the nature of the work-flow at our institution, it was not always possible to have patients on the same PET/CT scanner during both imaging sessions, and the use of two different scanners may have increased the measured variability. However, as noted in the supplemental material, both scanners that were utilized in this study are calibrated to provide the same SUVs, decreasing the likelihood that a significant portion of normal organ uptake variability is a result of imaging on different scanners. Lastly, while this study provides important information on normal organ uptake variability between scans in individual patients, it is not a true test-retest study. Rather, this is a more pragmatic attempt at quantifying organ uptake variability in a clinically relevant cohort of patients such as might be encountered in any

busy PCa oncology practice setting, and the reported levels of variability in this study are almost certainly higher than would be seen in a study in which factors such as current therapy are controlled for

Conclusions

Normal organs demonstrate significant variability in uptake of the PSMA-targeted radiotracer [^{18}F]DCFPyL. Depending on the organ, different contributions of interpatient and intrapatient factors affect the intrinsic variability observed, with the liver and kidneys having the highest contributions from intrapatient variability and the spleen having the lowest. The 95 % confidence limits of repeatability (RCs) also vary significantly among the different organs and are highest for the lacrimal glands, kidneys, and spleen. These findings may have important implications for the design of clinical protocols and personalized dosimetry for PSMA-targeted endoradiotherapies, although significant further study is required.

Supplementary Material

Refer to Web version on PubMed Central for supplementary material.

Funding

This project received funding from Progenics Pharmaceuticals, The Prostate Cancer Foundation Young Investigator Award, and National Institutes of Health grants CA134675, CA183031, CA184228, and EB024495. This project has received funding from the European Union's Horizon 2020 research and innovation program under the Marie Sklodowska-Curie grant agreement No 701983.

References

1. Rowe SP, Gorin MA, Allaf ME, Pienta KJ, Tran PT, Pomper MG, Ross AE, Cho SY (2016) PET imaging of prostate-specific membrane antigen in prostate cancer: current state of the art and future challenges. Prostate Cancer Prostatic Dis 19:223–230 [PubMed: 27136743]
2. Schwarzenboeck SM, Rauscher I, Bluemel C, Fendler WP, Rowe SP, Pomper MG, Asfhar-Oromieh A, Herrmann K, Eiber M (2017) PSMA ligands for PET imaging of prostate cancer. J Nucl Med 58:1545–1552 [PubMed: 28687599]
3. Perera M, Papa N, Christidis D, Wetherell D, Hofman MS, Murphy DG, Bolton D, Lawrentschuk N (2016) Sensitivity, specificity, and predictors of positive (68)Ga-prostate-specific membrane antigen positron emission tomography in advanced prostate cancer: a systematic review and meta-analysis. Eur Urol 70:926–937 [PubMed: 27363387]
4. Mena E, Lindenberg ML, Shih JH, Adler S, Harmon S, Bergvall E, Citrin D, Dahut W, Ton AT, McKinney Y, Weaver J, Eclarinal P, Forest A, Afari G, Bhattacharyya S, Mease RC, Merino MJ, Pinto P, Wood BJ, Jacobs P, Pomper MG, Choyke PL, Turkbey B (2018) Clinical impact of PSMA-based ^{18}F-DCFBC PET/CT imaging in patients with biochemically recurrent prostate cancer after primary local therapy. Eur J Nucl Med Mol Imaging 45:4–11 [PubMed: 28894899]
5. Calais J, Fendler WP, Eiber M, Gartmann J, Chu FI, Nickols NG, Reiter RE, Rettig MB, Marks LS, Ahlering TE, Huynh LM, Slavik R, Gupta P, Quon A, Allen-Auerbach MS, Czernin J, Herrmann K (2018) Impact of ^{68}Ga-PSMA-11 PET/CT on the management of prostate cancer patients with biochemical recurrence. J Nucl Med 59:434–441 [PubMed: 29242398]
6. Han S, Woo S, Kim YJ, Suh CH (2018) Impact of ^{68}Ga-PSMA PET on the management of patients with prostate cancer: a systematic review and meta-analysis. Eur Urol 74:179–190 [PubMed: 29678358]

7. Weineisen M, Schottelius M, Simecek J, Baum RP, Yildiz A, Beykan S, Kulkarni HR, Lassmann M, Klette I, Eiber M, Schwaiger M, Wester HJ (2015) ^{68}Ga- and ^{177}Lu-labeled PSMA I&T: optimization of a PSMA-targeted theranostic concept and first proof-of-concept human studies. J Nucl Med 56:1169–1176 [PubMed: 26089548]
8. Kabasakal L, AbuQbeitah M, Aygun A et al. (2015) Pre-therapeutic dosimetry of normal organs and tissues of ^{177}Lu-PSMA-617 prostate-specific membrane antigen (PSMA) inhibitor in patients with castration-resistant prostate cancer. Eur J Nucl Med Mol Imaging 42:1976–1983 [PubMed: 26227531]
9. Kulkarni HR, Singh A, Langbein T et al. (2018) Theranostics of prostate cancer: from molecular imaging to precision molecular radiotherapy targeting the prostate specific membrane antigen. Br J Radiol 20180308 [PubMed: 29762048]
10. Wahl RL, Jacene H, Kasamon Y, Lodge MA (2009) From RECIST to PERCIST: evolving considerations for PET response criteria in solid tumors. J Nucl Med 50(Suppl 1):122S–150S [PubMed: 19403881]
11. Li X, Rowe SP, Leal JP, Gorin MA, Allaf ME, Ross AE, Pienta KJ, Lodge MA, Pomper MG (2017) Semiquantitative parameters in PSMA-targeted PET imaging with ^{18}F-DCFPyL: variability in normal-organ uptake. J Nucl Med 58:942–946 [PubMed: 27932557]
12. Wondergem M, van der Zant FM, Vlottes PW, Knol RJJ (2018) Effects of fasting on ^{18}F-DCFPyL uptake in prostate cancer lesions and tissues with known high physiologic uptake. J Nucl Med 59:1081–1084 [PubMed: 29496983]
13. Ravert HT, Holt DP, Chen Y, Mease RC, Fan H, Pomper MG, Dannals RF (2016) An improved synthesis of the radiolabeled prostate-specific membrane antigen inhibitor, [^{18}F]DCFPyL. J Label Comp Radiopharm 59:439–450
14. Chen Y, Pullambhatla M, Foss CA, Byun Y, Nimmagadda S, Senthamizhchelvan S, Sgouros G, Mease RC, Pomper MG (2011) 2-(3-{1-Carboxy-5-[(6-[^{18}F]fluoro-pyridine-3-carbonyl)-amino]-pentyl}-ureido)-pen tanedioic acid, [^{18}F]DCFPyL, a PSMA-based PET imaging agent for prostate cancer. Clin Cancer Res 17:7645–7653 [PubMed: 22042970]
15. Rowe SP, Vicente E, Anizan N, Wang H, Leal JP, Lodge MA, Frey EC, Wahl RL (2015) Repeatability of radiotracer uptake in normal abdominal organs with ^{111}In-pentetreotide quantitative SPECT/CT. J Nucl Med 56:985–988 [PubMed: 25977467]
16. Shrout PE, Fleiss JL (1979) Intraclass correlations: uses in assessing rater reliability. Psychol Bull 86:420–428 [PubMed: 18839484]
17. Landis JR, Koch GG (1977) The measurement of observer agreement for categorical data. Biometrics 33:159–174 [PubMed: 843571]
18. Heijmen L, de Geus-Oei LF, de Wilt JH et al. (2012) Reproducibility of functional volume and activity concentration in ^{18}F-FDG PET/CT of liver metastases in colorectal cancer. Eur J Nucl Med Mol Imaging 39:1858–1867 [PubMed: 22945372]
19. Lodge MA (2017) Repeatability of SUV in oncologic ^{18}F-FDG PET. J Nucl Med 58:523–532 [PubMed: 28232605]
20. Kumar V, Nath K, Berman CG, Kim J, Tanvetyanon T, Chiappori AA, Gatenby RA, Gillies RJ, Eikman EA (2013) Variance of SUVs for FDG-PET/CT is greater in clinical practice than under ideal study settings. Clin Nucl Med 38:175–182 [PubMed: 23354032]
21. Weber WA, Gatsonis CA, Mozley PD, Hanna LG, Shields AF, Aberle DR, Govindan R, Torigian DA, Karp JS, Yu JQ, Subramaniam RM, Halvorsen RA, Siegel BA, ACRIN 6678 Research team, MK-0646–008 Research team (2015) Repeatability of ^{18}F-FDG PET/CT in advanced non-small cell lung cancer: prospective assessment in 2 multicenter trials. J Nucl Med 56:1137–1143 [PubMed: 25908829]
22. Giesel FL, Hadaschik B, Cardinale J, Radtke J, Vinsensia M, Lehnert W, Kesch C, Tolstov Y, Singer S, Grabe N, Duensing S, Schäfer M, Neels OC, Mier W, Haberkorn U, Kopka K, Kratochwil C (2017) F-18 labelled PSMA-1007: biodistribution, radiation dosimetry and histopathologic validation of tumor lesions in prostate cancer patients. Eur J Nucl Med Mol Imaging 44:678–688 [PubMed: 27889802]

Fig. 1.
Typical biodistribution of the majority of PSMA-targeted PET radiotracers, in this case [^{18}F]DCFPyL. For this study, organs with moderate-to-high uptake were selected including the lacrimal glands, salivary glands, liver, spleen, and kidneys.

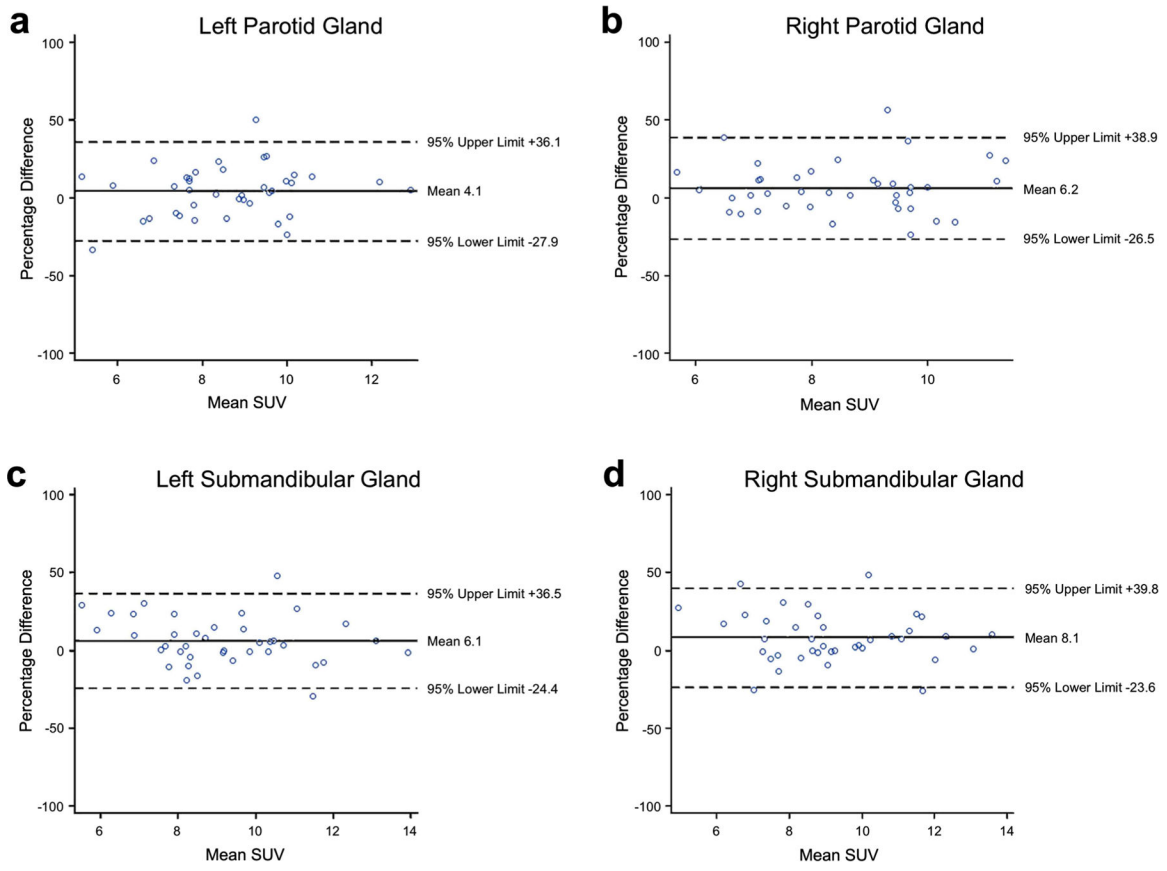

Fig. 2.

Variations in salivary gland uptake on [^{18}F]DCFPyL PET. Bland-Altman plots with the percentage difference in average uptake (SUV_{mean}) on the second scan as a function of the average uptake (SUV_{mean}) on the first scan: **a** left parotid, **b** right parotid, **c** left submandibular, and **d** right submandibular.

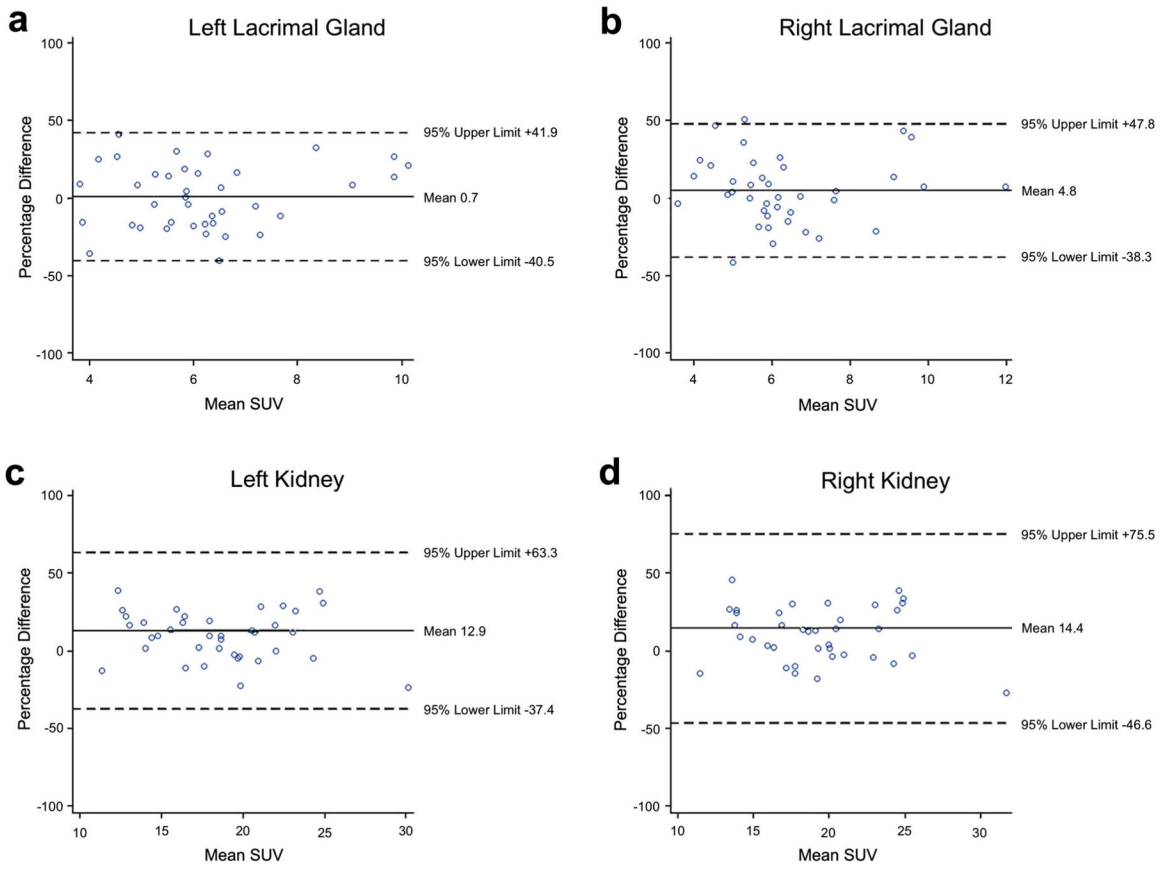

Fig. 3.

Variations in other paired organ (lacrimal gland and kidney) average radiotracer uptake. Bland-Altman plots with the percentage difference in average uptake (SUV_{mean}) on the second scan as a function of the average uptake (SUV_{mean}) on the first scan: **a** left lacrimal, **b** right lacrimal, **c** left kidney, and **d** right kidney.

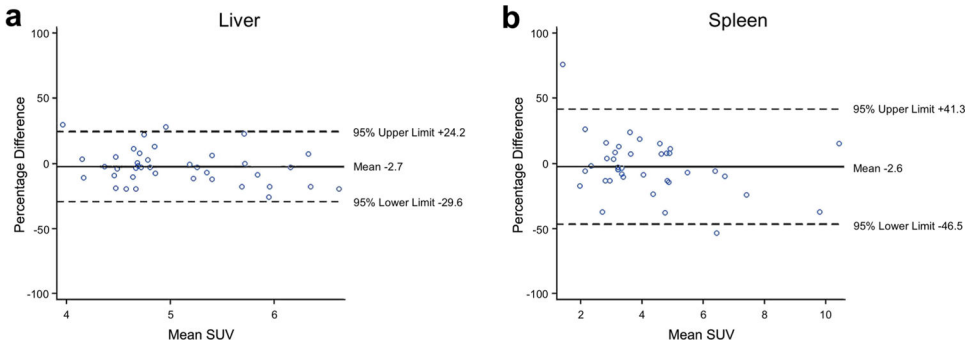

Fig. 4.

Variations in unpaired abdominal organ (liver and spleen) average radiotracer uptake. Bland-Altman plots with the percentage difference in average uptake (SUV_{mean}) on the second scan as a function of the average uptake (SUV_{mean}) on the first scan: **a** liver and **b** spleen).

Table 1.

Mean SUVs for each organ at baseline and at follow-up imaging

Organ	SUV mean at baseline	SUV mean at follow-up	*p* value
Right kidney	20.4 ± 4.7	18.6 ± 5.1	0.005
Left kidney	19.6 ± 4.5	17.8 ± 4.5	0.001
Liver	5.0 ± 0.7	5.2 ± 0.9	0.152
Spleen	4.1 ± 1.8	4.3 ± 2.2	0.144
Right lacrimal gland	6.5 ± 2.0	6.2 ± 1.8	0.179
Left lacrimal gland	6.2 ± 1.9	6.2 ± 1.5	0.638
Right parotid gland	8.8 ± 1.8	8.2 ± 1.6	0.030
Left parotid gland	8.8 ± 1.9	8.4 ± 1.6	0.076
Right submandibular gland	9.6 ± 2.1	8.9 ± 2.1	0.004
Left submandibular gland	9.4 ± 2.0	8.9 ± 2.1	0.037

Mol Imaging Biol. Author manuscript; available in PMC 2021 March 13.

Table 2.

Parameters of interpatient (COV) and intrapatient (ICC) variability at baseline and follow-up study

Organ	COV at baseline (%)	COV at follow-up (%)	ICC
Right kidney	23.1	30.0	0.40
Left kidney	22.9	28.2	0.50
Liver	13.0	16.6	0.57
Spleen	44.6	51.0	0.86
Right lacrimal gland	31.3	29.0	0.72
Left lacrimal gland	30.0	24.6	0.72
Right parotid gland	19.9	19.4	0.58
Left parotid gland	21.7	19.6	0.69
Right submandibular gland	22.2	23.8	0.73
Left submandibular gland	21.2	23.8	0.74

Mol Imaging Biol. Author manuscript; available in PMC 2021 March 13.

Table 3.

Mean percentage changes of SUV_{mean} with 95 % confidence limits for the organs included in this study as derived from Bland-Altman analysis

Organ	Mean change in SUV between baseline and follow-up scans (%)	95 % confidence upper limit (%)	95 % confidence lower limit (%)
Right kidney	+9.9	+45.0	−25.2
Left kidney	+10.1	+41.3	−21.1
Liver	−2.7	+24.2	−29.6
Spleen	−2.6	+41.3	−46.5
Right lacrimal gland	+4.8	+47.8	−38.3
Left lacrimal gland	+0.7	+41.9	−40.5
Right parotid gland	+6.2	+38.9	−26.5
Left parotid gland	+4.1	+36.1	−27.9
Right submandibular gland	+8.1	+39.8	−23.6
Left submandibular gland	+6.1	+36.5	−24.4

Mol Imaging Biol. Author manuscript; available in PMC 2021 March 13.